Inorganic Chemistry
Article

Inorg. Chem. **2010**, *49*, 4343–4354 **4343**
DOI: 10.1021/ic100313j

Mechanistic Studies on the Interaction of $[(\kappa^3\text{-}P,P,P\text{-}NP_3)IrH_3]$ $[NP_3 = N(CH_2CH_2PPh_2)_3]$ with HBF_4 and Fluorinated Alcohols by Combined NMR, IR, and DFT Techniques

Andrea Rossin,[†] Evgenii I. Gutsul,[‡] Natalia V. Belkova,[*,‡] Lina M. Epstein,[‡] Luca Gonsalvi,[†] Agustí Lledós,[*,§] Konstantin A. Lyssenko,[‡] Maurizio Peruzzini,[*,†] Elena S. Shubina,[*,‡] and Fabrizio Zanobini[†]

[†]*Instituto di Chimica dei Composti Organometallici* (*ICCOM-CNR*), *Via Madonna del Piano 10, 50019 Sesto Fiorentino* (*Firenze*), *Italy*, [‡]*A. N. Nesmeyanov Institute of Organoelement Compounds, Russian Academy of Sciences* (*INEOS-RAS*), *Vavilov strasse 28, 119991 Moscow, Russian Federation, and* [§]*Departament de Química, Universitat Autònoma de Barcelona, Bellaterra, Barcelona, Spain*

Received February 15, 2010

The novel iridium(III) hydride $[(\kappa^3\text{-}P,P,P\text{-}NP_3)IrH_3]$ $[NP_3 = N(CH_2CH_2PPh_2)_3]$ was synthesized and characterized by spectroscopic methods and X-ray crystallography. Its reactivity with strong (HBF_4) and medium-strength [the fluorinated alcohols 1,1,1-trifluoroethanol (TFE) and 1,1,1,3,3,3-hexafluoroisopropanol (HFIP)] proton donors was investigated through low-temperature IR and multinuclear NMR spectroscopy. In the case of the weak acid TFE, the only species observed in the 190−298 K temperature range was the dihydrogen-bonded adduct between the hydride and the alcohol, while with the stronger acid HBF_4, the proton transfer was complete, giving rise to a new intermediate $[(\kappa^3\text{-}P,P,P\text{-}NP_3)IrH_4]^+$. With a medium-strength acid like HFIP, two different sets of signals for the intermediate species were observed besides dihydrogen bond formation. In all cases, the final reaction product at ambient temperature was found to be the stable dihydride $[(\kappa^4\text{-}NP_3)IrH_2]^+$, after slow molecular dihydrogen release. The nature of the short-living species was investigated with the help of density functional theory calculations at the M05-2X//6-31++G(df,pd) level of theory.

Introduction

Hydrogen bonding and proton transfer to organometallic complexes, especially to transition-metal hydrides, as proton acceptors have attracted considerable attention in the recent decade.[1−3] Transition-metal complexes often bear ligands potentially capable of acting as proton donors or proton acceptors in hydrogen bonding. These functionalities are used to fine-tune the complex properties in catalysis or in molecular recognition and supramolecular assembly design.[4,5] If formed, the hydrogen bonds with these ligands would be qualitatively similar to those in traditional organic hydrogen complexes. On the other hand, core transition metals are able to accept a hydrogen bond through their d lone pairs, forming M···HA hydrogen bonds.[6] Hydride ligands possessing a partly negative charge, if present, are unusual proton-accepting sites, forming a so-called dihydrogen bond (DHB), M−H···HA.[1,4] These two types of hydrogen bonding, M···HA and M−H···HA, are unique for transition-metal (hydride) complexes, and the terms "nonclassical" or "unconventional" hydrogen bonding have been coined to address these interactions.[2] Thus, the dichotomy between different sites of proton donor attacks, classical and nonclassical, could arise for transition-metal complexes.

Another important aspect of a proton donor interaction with a transition-metal hydride is the structure of the dihydrogen-bonded complex formed. Our most recent study of hydrogen bonding with the hydride complexes $[Cp^*MH_3(dppe)]$ [M = Mo, W; dppe = 1,2-bis(diphenylphosphino)ethane; $Cp^* = \eta^5\text{-}C_5Me_5$] revealed the delicate balance of the M−H···HA and M···HA interactions within the same hydrogen complex (Scheme 1).[7,8]

The prevalence of either of the interactions apparently determines the hydride reactivity: M−H···HA bonding

*To whom correspondence should be addressed. E-mail: nataliabelk@ineos.ac.ru (N.V.B.), agusti@klingon.uab.es (A.L.), mperuzzini@iccom.cnr.it (M.P.), shu@ineos.ac.ru (E.S.S.).

(1) Belkova, N. V.; Shubina, E. S.; Epstein, L. M. *Acc. Chem. Res.* **2005**, *38*, 624.
(2) Peruzzini, M.; Poli, R. *Recent Advances in Hydride Chemistry*; Elsevier SA: Amsterdam, The Netherlands, 2001.
(3) Besora, M.; Lledós, A.; Maseras, F. *Chem. Soc. Rev.* **2009**, *38*, 957.
(4) Brammer, L. *Dalton Trans.* **2003**, 3145.
(5) Das, S.; Brudvig, G. W.; Crabtree, R. H. *Chem. Commun.* **2008**, 413.
(6) (a) Shubina, E. S.; Belkova, N. V.; Epstein, L. M. *J. Organomet. Chem.* **1997**, *536*−*537*, 17. (b) Epstein, L. M.; Shubina, E. S. *Coord. Chem. Rev.* **2002**, *231*, 165.
(7) Belkova, N. V.; Besora, M.; Baya, M.; Dub, P. A.; Epstein, L. M.; Lledós, A.; Poli, R.; Revin, P. O.; Shubina, E. S. *Chem.—Eur. J.* **2008**, *14*, 9921.
(8) Belkova, N. V.; Revin, P. O.; Besora, M.; Baya, M.; Epstein, L. M.; Lledós, A.; Poli, R.; Shubina, E. S.; Vorontsov, E. V. *Eur. J. Inorg. Chem.* **2006**, 2192.

Published on Web 04/08/2010

Scheme 1. Simplified Scheme of the Transition-Metal Hydride−Acid Interaction

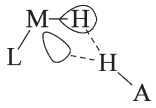

prevails for molybdenum, entailing $[Cp^*Mo(\eta^2\text{-}H_2)H_2(dppe)]^+$ complex formation, whereas M···HA bonding wins in the case of electron richer tungsten, where proton transfer yields directly the classical tetrahydride product $[Cp^*WH_4(dppe)]^+$. In the search for other experimental examples for such interactions with hydrides of the third-row transition metals, we carried out synthesis and protonation studies of the iridium hydride $[(\kappa^3\text{-}P,P,P\text{-}NP_3)IrH_3]$ [**3**; $NP_3 = N(CH_2CH_2PPh_2)_3$] presented herein. The potentially tetradentate aminotriphosphane tripodal ligand $N(CH_2CH_2PPh_2)_3$ offers diversity of coordination geometries because it may act as κ^4, κ^3-P_3, κ^3-N,P,P, and κ^2-P,P ligands.[9−11] The presence of the amine N donor and of two CH_2 spacers separating the P donors from the bridgehead atom makes NP_3 more flexible than other tripodal polyphosphines, e.g., $MeC(CH_2PPh_2)_3$, and also increases the overall basicity at the metal center.[9,10,12] In addition to the hydride ligand and the metal, the bridgehead N atom of NP_3 is also a potential protonation site, although examples of N-protonation are almost unknown in transition-metal complexes with this tripodal ligand.[13] A different behavior has been observed for other aminophosphines. Thus, protonation studies of ruthenium half-sandwich hydride complexes $[Cp^RRuH(P,N)]$ (Cp^R = Cp, Cp*) with bidentate *P*,*N*-aminophosphane ligands have shown that when stoichiometric amounts of HBF_4 are used, only the hydride is protonated, yielding the dihydrogen tautomer $[Cp^RRu(\eta^2\text{-}H_2)(P,N)]^+$ at low temperatures and dihydride tautomer $[Cp^RRu(H)_2(P,N)]^+$ upon warming. In contrast, reaction with an excess of HBF_4 affords the dicationic dihydride complexes $[Cp^RRu(H)_2(P,N-H)]^{2+}$ from protonation of both the hydride and the N lone pair.[14] The presence of three hydrides and a third-row transition metal and the coordinative flexibility of the aminophosphane ligand make **3** a suitable system for exploring its interaction with proton donors of different strength.

Experimental Section

All reactions were performed using the standard Schlenk procedures under a dry nitrogen or argon atmosphere, unless specified. The NP_3 ligand[15] and $[Ir(COD)Cl]_2$[16] (COD = 1,5-cyclooctadiene) were prepared according to published procedures. All solvents were purified by standard distillation techniques. 1,1,1,3,3,3-Hexafluoroisopropanol (HFIP), 1,1,1-trifluoroethanol (TFE), $HBF_4\cdot OMe_2$ (1:1 solution in OMe_2), and HOTf (OTf = trifluoromethanesulfonate, OSO_2CF_3) were used as purchased (Aldrich), without further purification. Deuterated solvents (Aldrich) were degassed by three freeze−pump−thaw cycles before use. NMR spectra were recorded on a Bruker AVANCE II 300 spectrometer, equipped with a low-temperature measurement tool. ^1H NMR chemical shifts are reported in parts per million (ppm) downfield of tetramethylsilane and were calibrated against the residual protiated resonance of the deuterated solvent, while $^{31}P\{^1H\}$ and ^{31}P NMR were referenced to 85% H_3PO_4 with the downfield shift taken as positive. ^{11}B NMR was referenced to $BF_3\cdot OEt_2$. The IR spectra were recorded on an FT Infralum-801 spectrometer. All measurements were carried out by use of a home-modified cryostat (Carl Zeiss Jena) in the 190−290 K temperature range. The cryostat modification allows operation under an inert atmosphere and transfer of the reagents (premixed either at low or room temperature) directly into the cell precooled to the required temperature. The accuracy of the temperature adjustment was ±1 K.

Synthesis of $[(\kappa^4\text{-}NP_3)IrCl]$ (1). A total of 335 mg (0.5 mmol) of $[Ir(COD)Cl]_2$ was dissolved in 35 mL of THF. A total of 653 mg of solid NP_3 (1 mmol) was added to this solution under stirring, and the mixture was stirred at room temperature, until a crystalline brick-red powder started to precipitate out. The supernatant was then filtered off, and the solid residue was washed with fresh THF (2 × 10 mL) and *n*-pentane (2 × 10 mL) and dried under a nitrogen stream. Yield: 80%. Anal. Calcd for $C_{42}H_{42}ClIrNP_3$: C, 57.23; H, 4.80; N, 1.59. Found: C, 57.06; H, 4.82; N, 1.52. The compound is insoluble in all solvents; therefore, no NMR characterization could be obtained.

Synthesis of $[(\kappa^4\text{-}NP_3)Ir(H)Cl]BPh_4$ (2). A total of 100 mg of **1** (0.1 mmol) was suspended in 20 mL of THF. A total of 50 mg (0.3 mmol) of pure HOTf was added to this suspension at room temperature under stirring, and the solid slowly started to dissolve to give a colorless solution. The mixture was stirred until complete dissolution of the reagent. At this stage, 200 mg of $NaBPh_4$ (0.6 mmol) dissolved in 15 mL of EtOH was then added to the initial mixture, and the final solution was concentrated under a nitrogen stream until a white precipitate of **2** formed. The supernatant was filtered off, and the solid was washed with fresh EtOH (2 × 10 mL) and *n*-pentane (2 × 10 mL) and dried under a nitrogen current. Yield: 78%. IR (Nujol, cm^{-1}): ν(Ir−H) 2100 s. ^1H NMR (300.13 MHz, ppm, $CDCl_3$): −10.34 (Ir−H, dt, $^2J_{H-P(trans)}$ = 149.8 Hz; $^2J_{H-P(cis)}$ = 15.2 Hz). $^{31}P\{^1H\}$ NMR (121.49 MHz, ppm, AM_2 spin system, $CDCl_3$): 1.33 (P_M, d, $^2J_{P-P}$ = 13.5 Hz), −9.45 (P_A, t). ^{11}B NMR (96.29 MHz, ppm, $CDCl_3$): −6.6 (br s). Anal. Calcd for $C_{66}H_{63}BClIrNP_3$: C, 65.96; H, 5.20; N, 1.16. Found: C, 65.48; H, 5.65; N, 1.06.

Synthesis of $[(\kappa^3\text{-}P,P,P\text{-}NP_3)IrH_3]$ (3). A total of 400 mg of **2** (0.3 mmol) was dissolved in 40 mL of THF. At room temperature, 400 mg of solid $LiAlH_4$ (10 mmol) is slowly added to this solution under vigorous stirring. When the addition was complete, the mixture was gently heated to the boiling point and then refluxed for 3.5 h. The reaction flask was then cooled at room temperature, and 11 mL of a H_2O/THF mixture (1:10) was carefully added in small portions in order to hydrolyze the excess of $LiAlH_4$. The supernatant was then filtered off, and the resulting clear solution was concentrated under a brisk stream of nitrogen. Further EtOH addition and concentration under nitrogen caused an off-white powder of **3** to precipitate from the solution. The crude compound was collected by filtration and washed with EtOH (2 × 5 mL) and *n*-pentane (10 mL) before being recrystallized from THF/EtOH (1:1). Yield: 72%. IR (CH_2Cl_2, 290 K, cm^{-1}): ν(Ir−H) 2040 (s). ^1H NMR (300.13 MHz, ppm, CD_2Cl_2): −12.24 (Ir−H, m, AA′A″XX′X″ spin system), 2.11 [CH_2 close to a P atom, s(br)], 2.97 [CH_2 close to a N atom, s(br)], 7.19−7.68 (aromatic CH, m). $^{31}P\{^1H\}$ NMR

(9) (a) Sacconi, L.; Mani, F. *Transition Met. Chem.* (*N.Y.*) **1982**, *8*, 214. (b) Sacconi, L.; Bertini, I. *J. Am. Chem. Soc.* **1968**, *90*, 5443. (c) Sacconi, L. *Coord. Chem. Rev.* **1972**, *8*, 351. (d) Morassi, R.; Bertini, I.; Sacconi, L. *Coord. Chem. Rev.* **1973**, *11*, 343. (e) Bertolasi, V.; Bianchini, C.; de los Ríos, I.; Marvelli, L.; Peruzzini, M.; Rossi, R. *Inorg. Chim. Acta* **2002**, *327*, 140–146.
(10) Mealli, C.; Ghilardi, C. A.; Orlandini, A. *Coord. Chem. Rev.* **1992**, *120*, 361.
(11) Palacios, M. D.; Puerta., M. C.; Valerga, P.; Lledós, A.; Veilly, E. *Inorg. Chem.* **2007**, *46*, 6958.
(12) Bianchini, C.; Meli, A.; Peruzzini, M.; Vizza, F.; Zanobini, F. *Coord. Chem. Rev.* **1992**, *120*, 193.
(13) A unique example of protonation at the N atom in NP_3 metal complexes has been reported. See: Cecconi, F.; Ghilardi, C. A.; Innocenti, P.; Mealli, C.; Midollini, S.; Orlandini, A. *Inorg. Chem.* **1984**, *23*, 922.
(14) Jiménez-Tenorio, M.; Palacios, M. D.; Puerta, M. C.; Valerga, P. *Inorg. Chem.* **2007**, *46*, 1001.
(15) Sacconi, L.; Bertini, I. *J. Am. Chem. Soc.* **1968**, *90*, 5443.
(16) Herde, J. L.; Lambert, J. C.; Senoff, C. V. *Inorg. Synth.* **1974**, *15*, 18.

Table 1. Crystal Data and Structure Refinement Parameters for **3** and **5**

	3	**5**
CCDC	713236	713237
formula	$C_{42}H_{45}IrNP_3$	$C_{42\cdot50}H_{45}BClF_4IrNP_3$
fw	848.90	977.17
T	100	100
cryst syst	monoclinic	monoclinic
space group, Z	$P2_1/c$, 4	$P2_1/n$, 4
a (Å)	10.3882(8)	9.8444(10)
b (Å)	8.3745(6)	27.254(4)
c (Å)	41.369(2)	15.109(2)
β (deg)	90.523(3)	105.211(3)
V (Å^3)	3598.8(4)	3911.6(9)
D_{calc} (g cm^{-1})	1.567	1.659
μ (cm^{-1})	38.75	36.56
$F(000)$	1704	1948
θ range (deg)	58	58
no. of reflns measd	76 022	63 497
no. of indep reflns (R_{int})	9568 (0.0495)	10 415 (0.0468)
no. of obsd reflns [$I > 2\sigma(I)$]	8697	8825
no. of param	436	493
final $R(F_{hkl})$:		
R1	0.0355	0.0363
wR2	0.0666	0.0965
GOF	1.081	0.996
$\Delta\rho_{max}$, $\Delta\rho_{min}$ (e Å^{-3})	1.339/−3.240	2.482/−1.896

(121.49 MHz, ppm, CD_2Cl_2): −12.12 (s). Anal. Calcd for $C_{42}H_{45}IrNP_3$: C, 59.42; H, 5.34; N, 1.65. Found: C, 59.76; H, 5.84; N, 1.55.

Synthesis of [(κ^4-NP_3)IrH_2] BF_4 (5). To 200 mg (0.2 mmol) of **3** suspended in 25 mL of THF was added via syringe 40 μL (0.3 mmol) of $HBF_4\cdot OMe_2$, causing slow dissolution of the starting trihydride after gentle warming of the solution with a water bath at 40 °C. The evolution of gaseous dihydrogen was also observed during the reaction. Concentration of the resulting clear solution under a stream of nitrogen gave a white crystalline precipitate of **5**, which was filtered and washed with degassed EtOH (2 × 10 mL) and *n*-pentane (2 × 10 mL) before being dried under nitrogen. Yield: 85%. IR (Nujol, cm^{-1}): ν(Ir−H) 2071 (s). ^{1}H NMR (300.13 MHz, ppm, CD_2Cl_2): −9.57 (Ir-H, H trans to P, br d, $^2J_{H-P(trans)}$ = 142.8 Hz), −18.50 (Ir-H, H trans to N, br s). $^{31}P\{^1H\}$ NMR (121.49 MHz, ppm, CD_2Cl_2): 18.50 (P trans to H, t, $^2J_{P-P}$ = 13.3 Hz), 20.11 (P trans to P, d). ^{11}B NMR (96.29 MHz, ppm, CD_2Cl_2): −0.64 (s). Anal. Calcd for $C_{42}H_{44}BF_4IrNP_3$: C, 67.91; H, 5.52; N, 1.20. Found: C, 67.74; H, 5.79; N, 1.14.

Variable-Temperature NMR Experiments on Hydride Protonation with HBF_4, HFIP, and TFE. A screw-cap NMR tube was loaded with 50 mg of **3** (0.06 mmol) under an inert atmosphere, and then 1 mL of dry and degassed CD_2Cl_2 was transferred into the tube via a cannula, under nitrogen. The suspension obtained was first used to record the $^{31}P\{^1H\}$, ^{1}H, ^{11}B, and $^1H\{^{31}P\}$ NMR spectra of the starting material at variable temperatures, by cooling of the sample in 20° steps from ambient conditions (300 K) to 190 K. The $^1H\{^{31}P\}$ T_1 values of **3** were also measured via the inversion−recovery sequence implemented on the software of the Bruker DRX spectrometer. A total of 7 μL of $HBF_4\cdot OMe_2$ (0.06 mmol) was syringed into this suspension kept at 195 K in a dry ice−acetone bath, and immediate dissolution was observed. The clear mixture was then transferred back into the NMR spectrometer (still at 190 K) and warmed stepwise to room temperature with the same procedure as that above. A new set of multinuclear NMR and $^1H\{^{31}P\}$ T_1 data were recorded during warming and following the reaction course. The reaction of **3** with TFE or HFIP was carried out and monitored in the same manner.

Crystallographic Studies. All diffraction data were taken using a Bruker SMART APEX II CCD diffractometer [λ(Mo Kα) = 0.710 72 Å, ω scans; see Table 1]. The substantial redundancy in the data allows empirical absorption correction to be applied using multiple measurements of equivalent reflections with the Bruker program *SADABS*. The structures were solved by direct methods and refined by the full-matrix least-squares technique against F^2 in the anisotropic−isotropic approximation. The hydrides were located from the Fourier density synthesis and refined within a riding model with fixed Ir−H distances equal to 1.640 Å, according to neutron data coming from the iridium complex *fac*-$IrH_3(PPh_2Me)_3$.[17] The positions of all of the other H atoms of the NP_3 ligand were located geometrically, and their thermal factors were related to the heavier atoms that they are bound to. Analysis of the Fourier density synthesis revealed that the BF_4^- anion in **5** is disordered by two positions with occupancies of 0.2 and 0.8. The disorder on the N atom of NP_3 in **1** (see the Supporting Information) was not explicitly treated because no significant improvement of the *R* factors was observed. All calculations were performed using the *SHELXTL* software.[18] The crystallographic data for **1**, **3**, and **5** have been deposited with the Cambridge Crystallographic Data Centre (CCDC nos. 769848, 713236, and 713237). The coordinates can be obtained, upon request, from the Director, Cambridge Crystallographic Data Centre, 12 Union Road, Cambridge CB2 1EZ, U.K.

Computational Details. All of the calculations were performed with the *Gaussian03* software package[19] at the density functional theory (DFT)/M05-2X level.[20] In order to have reasonable computational times, a model system obtained by replacing the phenyl groups on NP_3 with H atoms was used instead of the real molecule. Thus, all of the model complexes and intermediates contain the $N(CH_2CH_2PH_2)_3$ ligand, and they are indicated with the apex "t" on the corresponding numbers throughout the text. In the basis set employed for the geometry optimization procedure (BS1), core electrons of the Ir and P atoms were described using the pseudopotentials of Hay−Wadt,[21] and their valence electrons were expressed through a LANL2DZ basis set.[21] An extra p-type polarization function for the P atom and an extra f-type function for the Ir atom were added to the standard set.[22] A 6-31+G(d,p) basis set was used on the hydride ligands, while a 6-31G basis set was chosen for all of the other atoms. On the optimized structures, frequency calculations with a more extended basis set [BS2: same basis set on Ir and P atoms, 6-31++G(df,pd) on the hydride ligands, and 6-31+G(d,p) on all of the other atoms] were performed to calculate zero-point energies, enthalpies,

(17) Bau, R.; Schwerdtfeger, C. J.; Garlaschelli, L.; Koetzle, T. F. *J. Chem. Soc., Dalton Trans.* **1993**, 3359.
(18) *SHELXTL*, version 6.1; Bruker AXS Inc.: Madison, WI, **2005**.
(19) Frisch, M. J.; Trucks, G. W.; Schlegel, H. B.; Scuseria, G. E.; Robb, M. A.; Cheeseman, J. R.; Montgomery, J. A. J.; Vreven, T.; Kudin, K. N.; Burant, J. C.; Millam, J. M.; Iyengar, S. S.; Tomasi, J.; Barone, V.; Mennucci, B.; Cossi, M.; Scalmani, G.; Rega, N.; Petersson, G. A.; Nakatsuji, H.; Hada, M.; Ehara, M.; Toyota, K.; Fukuda, R.; Hasegawa, J.; Ishida, M.; Nakajima, T.; Honda, Y.; Kitao, O.; Nakai, H.; Klene, M.; Li, X.; Knox, J. E.; Hratchian, H. P.; Cross, J. B.; Adamo, C.; Jaramillo, J.; Gomperts, R.; Stratmann, R. E.; Yazyev, O.; Austin, A. J.; Cammi, R.; Pomelli, C.; Ochterski, J. W.; Ayala, P. Y.; Morokuma, K.; Voth, G. A.; Salvador, P.; Dannenberg, J. J.; Zakrzewski, V. G.; Dapprich, S.; Daniels, A. D.; Strain, M. C.; Farkas, O.; Malick, D. K.; Rabuck, A. D.; Raghavachari, K.; Foresman, J. B.; Ortiz, J. V.; Cui, Q.; Baboul, A. G.; Clifford, S.; Cioslowski, J.; Stefanov, B. B.; Liu, G.; Liashenko, A.; Piskorz, P.; Komaromi, I.; Martin, R. L.; Fox, D. J.; Keith, T.; Al-Laham, M. A.; Peng, C. Y.; Nanayakkara, A.; Challacombe, M.; Gill, P. M. W.; Johnson, B.; Chen, W.; Wong, M. W.; Gonzalez, C.; Pople, J. A. *Gaussian 03*, revision E.01; Gaussian, Inc.: Wallingford, CT, **2004**.
(20) Zhao, Y.; Schultz, N. E.; Truhlar, D. G. *J. Chem. Theor. Comput.* **2006**, *2*, 364.
(21) (a) Hay, P. J.; Wadt, W. R. *J. Chem. Phys.* **1985**, *82*, 270. (b) Wadt, W. R.; Hay, P. J. *J. Chem. Phys.* **1985**, *82*, 284.
(22) (a) Höllwarth, A.; Böhme, M.; Dapprich, S.; Ehlers, A. W.; Gobbi, A.; Jonas, V.; Köhler, K. F.; Stegmann, R.; Veldkamp, A.; Frenking, G. *Chem. Phys. Lett.* **1993**, *208*, 237. (b) Ehlers, A. W.; Böhme, M.; Dapprich, S.; Gobbi, A.; Höllwarth, A.; Jonas, V.; Köhler, K. F.; Stegmann, R.; Veldkamp, A.; Frenking, G. *Chem. Phys. Lett.* **1993**, *208*, 111.

Scheme 2

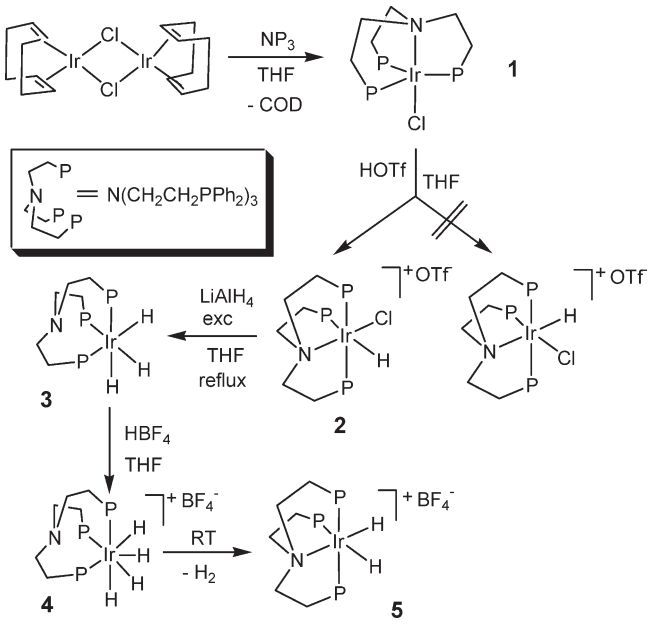

entropies, and gas-phase Gibbs energies at 298 K more accurately. Finally, a continuum modeling of the reaction medium was also included in the computational treatment, using BS2 on all of the BS1-level optimized structures. Bulk solvent effects (CH_2Cl_2, $\varepsilon = 8.93$) were expressed through the polarizable continuum model (PCM-UA0 solvation spheres).[23] Individual solvation cavities were added on the H atoms of the nonclassical η^2-H_2 ligand, when present.

Results and Discussion

Synthesis and Characterization of Compounds 1−3. The iridium NP_3 derivatives described in this paper (see Scheme 2) were prepared starting from the chloro compound **1**, obtained by the straightforward substitution of the labile COD ligand in $[Ir(COD)Cl]_2$ by the tripodal tetradentate ligand NP_3. Complex **1** was obtained as brick-red microcrystalline material air stable in the solid state. **1** is insoluble in both polar and apolar solvents; it shows a little solubility only in dichloromethane, where it decomposes in a short time. Consequently, any spectroscopic characterization in solution was precluded. As expected from the coordination abilities of tripodal polyphosphines, **1** exhibits a trigonal bipyramidal structure, as confirmed by independent crystallographic results.[24] The complex has a C_3 symmetry axis coincident with the N−Ir−Cl direction (Figure S1 and Tables S1−S2 in the Supporting Information); its hexagonal space group ($P6_3$) is chiral, with the optical activity being generated by the "propeller-like" orientation of the three NP_3 arms when they bind the iridium center. An interesting feature is the strong disorder of the N atom along the N−Ir direction, even at 150 K, which can be seen as proof of the coordination "flexibility" of the tripodal phosphine (easy $\kappa^4 \leftrightarrow \kappa^3$ coordination mode switch).

(23) (a) Miertus, S.; Scrocco, E.; Tomasi, J. *J. Chem. Phys.* **1981**, *55*, 117. (b) Barone, V.; Cossi, M.; Tomasi, J. *J. Chem. Phys.* **1997**, *107*, 3210.

(24) Complex **1** shares its geometric properties with the related tripodal polyphosphine complex $[(PP_3)IrCl]$. See: Bianchini, C.; Peruzzini, M.; Zanobini, F. *J. Organomet. Chem.* **1987**, *326*, C79.

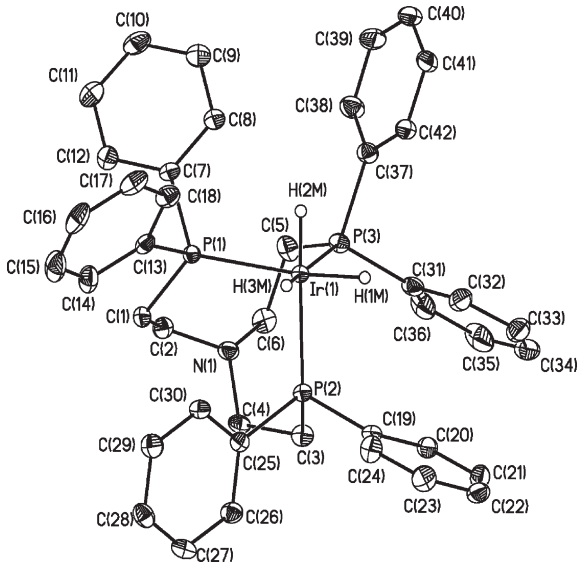

Figure 1. Molecular structure of **3** (50% probability level). All of the H atoms, apart the hydride ligands, are omitted for clarity. Selected bond lengths and angles are given in Table 2.

Protonation of **1** with a strong acid like HOTf in THF at room temperature, followed by triflate/tetraphenylborate anion exchange, leads to formation of the iridium(III) cationic species **2**, in good yield. Compound **2** shows an octahedral coordination geometry at iridium, with the NP_3 ligand being again tetradentate, as evidenced by the $^{31}P\{^1H\}$ NMR spectrum, where two different phosphorus resonances can be detected, with a 2:1 intensity ratio (AM_2 spin system). Turning off the ^1H decoupler in the ^{31}P NMR spectrum clearly splits the phosphorus resonance at −9.45 ppm ($^2J_{P-H(trans)} = 149.8$ Hz), then confirming that protonation takes place with complete stereoselectivity at the metal as the proton atom is exclusively delivered to the equatorial position cis to the N atom (see Scheme 2). In keeping with this stereochemical evidence, the ^1H NMR spectrum shows two temperature-invariant high-field triplets with similar separation that collapse to a singlet ($\delta = -10.34$ ppm) after decoupling the P_A resonance [$^1H\{^{31}P_A\}_{sel}$ experiment]. Treatment of **2** with a strong excess of $LiAlH_4$ in THF gives, after workup, off-white crystals of the neutral trihydride complex **3** in excellent yield. The iridium(III) trihydrido complex **3** is air-stable in the solid state and does not decompose in a THF solution, from which very pale-yellow crystals suitable for an X-ray diffraction analysis were grown, after standing overnight in the presence of EtOH.

A thermal ellipsoid representation of the solid-state structure of **3**, along with atomic numbering schemes, is depicted in Figure 1, whereas selected bond distances (Å) for **3** and **5** are provided in Table 2.

According to the single-crystal X-ray diffraction analysis, the Ir atom in **3** adopts a pseudooctahedral coordination geometry formed by the three P atoms of the tripodal ligand and three hydrides, without the N atom of the NP_3 ligand entering the metal coordination sphere (Figure 1). The Ir(1)···N(1) separation in **3** is 3.518(1) Å, with the N(1) atom deviating from the plane of the C(2), C(4), and C(6) atoms by 0.32 Å, pointing toward the metal. The observed pyramidalization of the N(1) atom is

Table 2. − Selected Bond Distances (Å) and Angles (deg) for Complexes **3** and **5**[a]

complex **3**	complex **5**
	Ir(1)−N(1) = 2.217(4)
	Ir(1)−P(1) = 2.3257(11)
Ir(1)−P(1) = 2.3403(9)	Ir(1)−P(2) = 2.3073(11)
Ir(1)−P(2) = 2.3162(9)	Ir(1)−P(3) = 2.2745(11)
Ir(1)−P(3) = 2.3362(9)	N(1)−C(2) = 1.513(6)
N(1)−C(2) = 1.449(5)	N(1)−C(4) = 1.505(5)
N(1)−C(4) = 1.455(5)	N(1)−C(6) = 1.512(5)
N(1)−C(6) = 1.464(5)	N(1)−Ir(1)−P(9) = 85.35(10)
P(9)−Ir(1)−P(4) = 99.98(3)	N(1)−Ir(1)−P(10) = 84.00(10)
P(9)−Ir(1)−P(10) = 99.93(3)	P(9)−Ir(1)−P(10) = 157.64(4)
P(4)−Ir(1)−P(10) = 99.61(3)	N(1)−Ir(1)−P(8) = 86.49(11)
	P(9)−Ir(1)−P(8) = 102.69(4)
	P(10)−Ir(1)−P(8) = 96.22(4)

[a] Refer to Figures 1 and 3 for atom numbering.

similar to that observed in the known κ^3-*P*,*P*,*P*-NP_3 complexes (0.29−0.4 Å), as are the N−C distances (of ca. 1.45 Å).[25]

The Ir(1)−P bonds are merely equal and slightly longer than those found in the related complex *fac*-[IrH_3-(PPh_2Me)$_3$] (2.308 Å).[17] There are short (less than the sum of van der Waals radii, 2.4 Å) intramolecular contacts between phenyl CH groups and hydride ligands [H(1M)···H(32A) = 2.07 Å, H(2M)···H(8A) = 1.97 Å, and H(3M)···H(30A) = 2.14 Å]. The crystal packing analysis revealed also that one of the hydride atoms of **3** is at a short distance to the CH_2 group: the H(3M)···H(6A) separation is equal to 2.07 Å (with normalization of the C−H bond to the ideal distance), and the corresponding CH···H and IrH···H angles are equal to 128 and 175°, respectively. Another close contact between the two adjacent molecules via phenyl CH pointing toward the hydride ligand is also present; CH···H(Ir) distance = 2.89 Å, angle = 169°. On the basis of geometrical parameters, we can suggest that these contacts correspond to weak intermolecular H···H hydrogen bonds.

Complex **3** has C_{3v} symmetry, which should give three ν_{Ir-H} vibrations in the IR spectrum.[26] Indeed, three ν_{Ir-H} bands are observed (at 2022 and 2036 cm^{-1} with a shoulder at 2055 cm^{-1}) in the solid-state spectrum. This splitting is lost in solution, where the broad ($\Delta\nu_{1/2}$ = 56 cm^{-1} at 290 K) asymmetric ν_{Ir-H} band is observed at 2040 cm^{-1} (ε_{Ir-H} = 570 L mol^{-1} cm^{-1}) in CH_2Cl_2. The position (ν_{Ir-H}), half-height at full width ($\Delta\nu_{1/2}$), and extinction coefficient (ε_{Ir-H}) for this band are temperature-dependent, being, at 190 K, 2025 cm^{-1}, 54 cm^{-1}, and 700 L mol^{-1} cm^{-1}, correspondingly. In other words, the band ascribed to the Ir−H stretching becomes more intense and shifts to lower frequency upon cooling (Figure S2 in the Supporting Information) as observed for other transition-metal hydrides [see the references in the Introduction section]. At room temperature, hydride **3** exhibits an AA′A″XX″X″ second-order ^1H NMR resonance in the hydride region centered at −12.2 ppm,

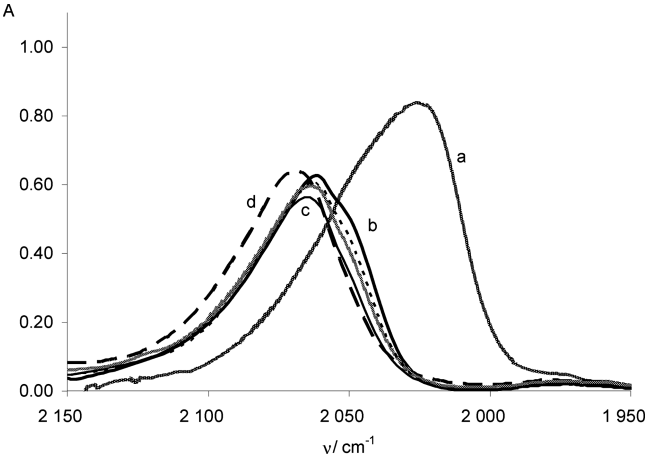

Figure 2. IR spectra (CH_2Cl_2, ν_{Ir-H} region) of **3** (0.006 M, a) in the presence of ca. 1.5 equiv of HBF_4 at 190 K (b) and 250 K (c) with the intermediate spectra at 210 and 230 K. (d) The spectrum of **5** (0.006 M) at 298 K is given for comparison.

while a singlet at −12.1 ppm is observed in the $^{31}P\{^1H\}$ NMR spectrum. The $^1H\{^{31}P\}$ NMR spectrum clearly reveals that the hydride signal multiplicity is due to P atoms only, ruling out any magnetic inequivalence of the three hydrido H atoms because a *singlet* is obtained when the ^{31}P coupling is turned off. Complex **3** is stereochemically rigid on the NMR time scale; neither the ^{31}P NMR spectrum nor the ^1H NMR spectrum shows significant changes over the temperature window of dichloromethane except for the slight drift of the signals with temperature (δ_{Ir-H} going from −12.2 to −12.4 ppm and δ_P going from −12.1 to −12.3 ppm at 298 and 190 K, respectively). The recorded values of the spin−lattice T_1 relaxation time (300 MHz, CD_2Cl_2) are typical of a *classical* polyhydride falling in the 200−450 ms range,[27] with a $T_{1,min}$ value of ca. 200 ms (at 223 K).

Protonation of 3 with Strong Protic Acids: HBF_4. Protonation of **3** in dichloromethane by the strong acid $HBF_4 \cdot OMe_2$ was followed by variable-temperature IR and NMR spectroscopies. Upon the low-temperature (190 K) addition of a slight excess of $HBF_4 \cdot OMe_2$, the ν_{Ir-H} band of **3** disappears and a new band appears at 2062 cm^{-1} with a shoulder at 2050 cm^{-1} (Figure 2). Such a high-frequency shift ($\Delta\nu_{Ir-H}$ = 37 cm^{-1}) is in line with the formation of a new cationic polyhydrido species [(κ^3-*P*,*P*,*P*-NP_3)IrH_4]$^+$ (**4**). No evidence of N-protonation on the ^1H NMR spectra was found, even after the addition of a large excess of acid (to a final 4:1 acid-to-complex stoichiometric ratio). This is probably due to both the "spatial shielding" offered by the dangling NP_3 arms and the particular N lone-pair orientation, pointing inward in the direction of the metal center and not outward (where it would be more exposed to electrophilic attacks).[10,13]

To establish the precise chemical nature of the new complex **4**, the reaction was also monitored by ^1H and $^{31}P\{^1H\}$ NMR spectroscopies at variable temperature. In agreement with the IR analysis, NMR signals of a new species were observed upon the addition of less than 1 equiv of HBF_4 to a CD_2Cl_2 solution of **3** at 190 K, besides those of the starting material. In the ^1H NMR spectrum, a new doublet of

(25) Examples of κ^3-*P*,*P*,*P*-NP_3 complexes characterized through X-ray diffraction include: (a) Dapporto, P.; Midollini, S.; Sacconi, L. *Angew. Chem., Int. Ed.* **1979**, *18*, 469. (b) Bianchini, C.; Meli, A.; Peruzzini, M.; Vizza, F.; Bachechi, F. *Organometallics* **1991**, *10*, 820. (c) Ghilardi, C. A.; Innocenti, P.; Midollini, S.; Orlandini, A.; Vacca, A. *J. Chem. Soc., Chem. Commun.* **1992**, 1691. (d) Barbaro, P.; Cecconi, F.; Ghilardi, C. A.; Midollini, S.; Orlandini, A.; Vacca, A. *Inorg. Chem.* **1994**, *33*, 6163.

(26) Nakamoto, K. *Infrared and Raman Spectra of Inorganic and Coordination Compounds*, 5th ed.; John Wiley & Sons Inc.: New York, 1997.

(27) Bakhmutov, V. I. *Practical NMR Relaxation for Chemists*; Wiley-VCH: New York, 2004.

triplets, centered at −11.1 ppm ($^2J_{H-P(trans)}$ = 121.5 Hz, $^2J_{H-P(cis)}$ = 17.5 Hz) comes out in the hydride region, while a new singlet appears in the $^{31}P\{^1H\}$ NMR spectrum (δ = −22.7 ppm). The $^1H\{^{31}P\}$ NMR signal exhibits a high-field singlet, thus indicating exclusive coupling with P atoms. The occurrence of a temperature-invariant singlet resonance in the ^{31}P NMR spectrum asks for the rapid H-atom exchange in **4**, while the magnetic nonequivalence of the P atoms is preserved during the scrambling process and, consequently, mirrored in the ^1H NMR spectrum. The T_1 values measured for this new compound are in the 200 ms to 1.5 s range, with the $T_{1,min}$ value of 200 ms at 243 K. Notably, the temperature corresponding to $T_{1,min}$ increases upon protonation from 223 to 243 K, whereas the $T_{1,min}$ value remains the same. This phenomenon agrees with a decreased correlation time (τ_C), related to a slower tumbling motion for the protonated species, as expected from its larger size.[27] Thus, this new species can be formulated as the cationic tetrahydrido complex **4** featuring a κ^3-coordination of the tripodal aminophosphine and a pentagonal-bipyramidal-coordination polyhedron around the metal. This geometrical assignment is supported by a comparison of the different NMR behavior of **4** with that of the known classical rhenium tetrahydride $[(\kappa^4\text{-}NP_3)ReH_4]^+$, for which a temperature-dependent $A_3 \rightarrow A_2M \rightarrow AMX$ change of the $^{31}P\{^1H\}$ NMR spectrum was observed to decrease with the temperature and a distorted dodecahedral eight-coordinated geometry was authenticated in the solid state by X-ray crystallography.[28]

Warming the solution of **4** initiates a subsequent slow transformation accompanied by dihydrogen evolution (evident from the appearance of the characteristic singlet resonance at 4.6 ppm). The transformation of **4** into the dihydrido complex **5** completes at 293 K when no residual resonances of either the tetrahydride or the starting material **3** are still present in the NMR spectrum. Complex **5** features an AM_2 $^{31}P\{^1H\}$ NMR pattern (δ_A = 18.5 ppm, t, $^2J_{P-P}$ = 13.3 Hz; δ_M = 20.1 ppm, d) and two distinct hydride resonances (δ_H = −9.6 ppm, br d, $^2J_{HP(trans\ to\ H)}$ = 142.8 Hz; δ_H = −18.5 ppm, br s). Interestingly, discernible couplings between the (chemically and magnetically) *nonequivalent* H and P atoms could *not* be observed when HBF_4 is used to protonate **4**. A much better spectral resolution was observed when weaker acids, such as HFIP, are used (vide infra). The IR spectra confirmed the NMR data: complex **5** generated in situ by the reaction of **3** with HBF_4 features a sharp ν_{Ir-H} band at 2071 cm^{-1} (ε = 480 L mol^{-1} cm^{-1}), which coincides with that of the isolated crystalline $[(\kappa^4\text{-}NP_3)IrH_2]BF_4$ salt isolated as off-white crystals from a bulk preparative reaction carried out in CH_2Cl_2. The presence of a κ^4-coordinated ligand in **5** is also indirect proof of the aforementioned absence of N-atom protonation, which could *not* coordinate to the iridium center if it had previously reacted with H^+.

The structure of **5** was unambiguously identified through single-crystal X-ray analysis carried out on crystalline samples of the compound prepared via an independent synthesis. Complex **5** also features the pseudooctahedral coordination geometry around iridium formed by all four donor atoms of the tripodal ligand and two cis-disposed hydrides (Figure 3 and Table 2). The Ir(1)−N(1) bond in **5** is almost equal to the corresponding value in the $[(\kappa^4\text{-}NP_3)IrH(\sigma\text{-}C_8H_{11})]^+$ cation.[29] Participation of the N atom in the coordination leads to some elongation of the N−C bonds from 1.449(5)−1.465(5) Å in **3** to 1.505(5)−1.513(6) Å in **5** as well as to an increase of the N-atom pyramidalization. Deviation of the N(1) atom from the plane of the C(2), C(4), and C(6) atoms becomes as much as 0.53 Å (vs 0.32 Å in **3**). The Ir(1)−P(2) and Ir(1)−P(3) bonds are slightly shortened to 2.274(1) and 2.307(1) Å. Finally, there is an extremely short intramolecular C−H···H−Ir separation between the H atom of the phenyl group and the hydride ligand, with the H(3M)···H(20A) distance being of 1.90 Å and C−H···H and Ir−H···H angles being 128 and 113°, respectively.

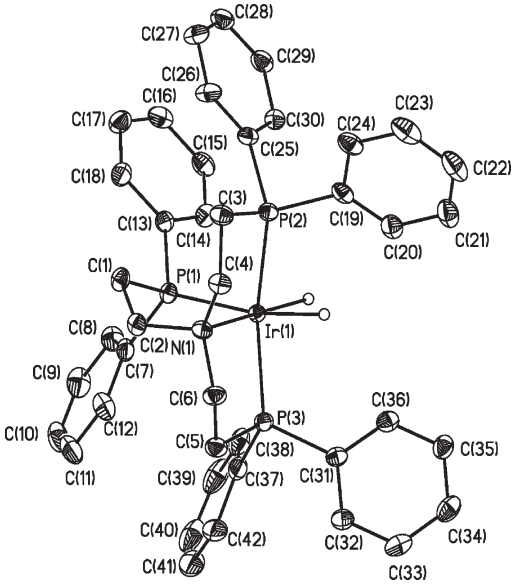

Figure 3. Molecular structure of the complex cation in **5** (50% probability level). All of the H atoms, apart from the hydride ligands, are omitted for clarity. Selected bond lengths and angles are given in Table 2.

Following our well-developed approach,[7,8,28,30] we decided to study the reaction mechanism of proton transfer to the trihydride **3** by using weaker proton donors, i.e., fluorinated alcohols of variable strength such as TFE and HFIP. These alcohols should indeed offer better reaction kinetics control with respect to stronger acids like HBF_4.

Reaction of 3 with TFE. As can be expected, interaction of hydride **3** with the least acidic TFE (pK_a = 12.5) did not lead to proton transfer. The addition of 5−20 equiv

(28) Albinati, A; Bakhmutov, V. I.; Belkova, N. V.; Bianchini, C.; de los Rios, I.; Epstein, L.; Gutsul, E. I.; Marvelli, L.; Peruzzini, P.; Rossi, R.; Shubina, E.; Vorontsov, E. V.; Zanobini, F. *Eur. J. Inorg. Chem.* **2002**, 1530.

(29) Bianchini, C.; Masi, D.; Meli, A.; Peruzzini, M.; Sabat, M.; Zanobini, F. *Organometallics* **1986**, *5*, 2557.

(30) (a) Shubina, E. S.; Belkova, N. V.; Bakhmutova, E. V.; Vorontsov, E. V.; Bakhmutov, V. I.; Ionidis, A. V.; Bianchini, C.; Marvelli, L.; Peruzzini, M.; Epstein, L. M. *Inorg. Chim. Acta* **1998**, *280*, 302. (b) Bakhmutov, V. I.; Bianchini, C.; Peruzzini, M.; Vizza, F.; Vorontsov, E. V. *Inorg. Chem.* **2000**, *39*, 1655. (c) Bakhmutov, V. I.; Bakhmutova, E. V.; Belkova, N. V.; Bianchini, C.; Epstein, L. M.; Peruzzini, M.; Shubina, E. S.; Vorontsov, E. V.; Zanobini, F. *Can. J. Chem.* **2001**, *79*, 479. (d) Gutsul, E. I.; Belkova, N. V.; Sverdlov, M. S.; Epstein, L. M.; Shubina, E. S.; Bakhmutov, V. I.; Gribanova, T. N.; Minyaev, R. M.; Bianchini, C.; Peruzzini, M.; Zanobini, F. *Chem.—Eur. J.* **2003**, *9*, 2219. (e) Gutsul, E. I.; Belkova, N. V.; Babakhina, G. M.; Epstein, L. M.; Shubina, E. S.; Bianchini, C.; Peruzzini, M.; Zanobini, F. *Russ. Chem. Bull. Int. Ed.* **2003**, *52*, 1204. (f) Bolaño, S.; Gonsalvi, L.; Barbaro, P.; Albinati, A.; Rizzato, S.; Gutsul, E.; Belkova, N.; Epstein, L.; Shubina, E.; Peruzzini, M. *J. Organomet. Chem.* **2006**, *691*, 629. (g) Belkova, N. V.; Gribanova, T. N.; Gutsul, E. I.; Minyaev, R. M.; Bianchini, C.; Peruzzini, M.; Zanobini, F.; Epstein, L. M.; Shubina, E. S. *J. Mol. Struct.* **2007**, *844/845*, 115.

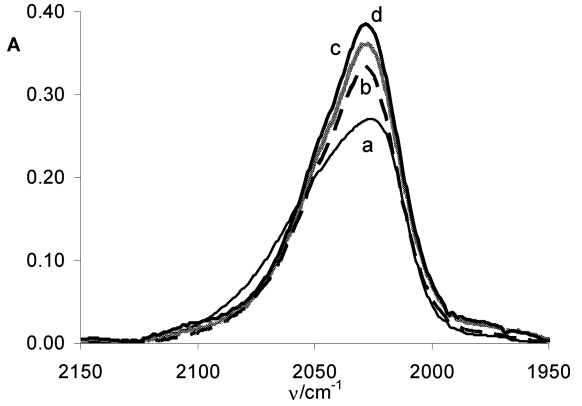

Figure 4. IR spectra (ν_{Ir-H} region) of **3** (0.01 M) in CH_2Cl_2 at 200 K in the presence of 0 equiv (a), 5 equiv (b), 10 equiv (c), 20 equiv (d) of TFE.

of TFE entails only the intensity increase of the ν_{Ir-H} band (Figure 4), which could be assigned to the formation of dihydrogen-bonded complex [IrH]···$HOCH_2CF_3$ (**3a**).[1,2,6−9,28,30]

In order to confirm this hypothesis, the $^{31}P\{^1H\}$ and ^1H NMR spectra of **3** were measured in CD_2Cl_2 in the presence of 6 equiv of TFE. At 190 K, the δ_{OH} value of TFE shifts considerably in the presence of **3**, passing from 2.9 ppm in the free alcohol to 5.6 ppm. This downfield shift of the acidic proton signal is in line with the hydrogen-bond formation. A new hydride signal appears at stronger field ($\delta = -12.6$ ppm; $\Delta\delta_H = -0.2$ ppm; see Figure S3 in the Supporting Information), while the "new" δ_P is observed at −13.7 ppm instead of −12.3 ppm. The $T_{1,min}$ value of 143 ms was found at 233 K for the hydride signal in the presence of TFE, which is 1.4 times lower than that of free hydride. Altogether, these observations evidence DHB formation.[1] No signals belonging to a different species (such as **4** or **5**) were detected on the NMR spectra in the entire temperature range up to 290 K; thus, neither proton transfer nor dihydrogen evolution takes place.

As previously reported for other similar systems,[30] the Ir−H···HOR distance can be estimated from the $T_{1\text{-min}}$ data. According to eq 1

$$1/T_{1,\mathrm{min}}{}^{\mathrm{obs}} = \frac{1}{3}[1/T_{1,\mathrm{min}}{}^{\mathrm{obs}}{}_{(\mathrm{IrH\cdots HOR})}] + \frac{2}{3}[1/T_{1,\mathrm{min(IrH_3)}}] \quad (1)$$

the observed $T_{1,min}{}^{obs}$ value was employed to calculate $T_{1,min}{}^{obs}{}_{(IrH\cdots HOR)}$ for the dihydrogen-bonded hydride ligand in **3a**. In turn, this value was used together with $T_{1,min}{}^{obs}{}_{(IrH3)}$ of complex **3** to calculate the $T_{1,min(H\cdots H)}$ value, which is exclusively due to hydride−proton dipole−dipole interactions (eq 2).

$$1/T_{1,\mathrm{min}}{}^{\mathrm{obs}}{}_{(\mathrm{IrH\cdots HOR})} = 1/T_{1,\mathrm{min(IrH)}} + 1/T_{1,\mathrm{min(H\cdots H)}} \quad (2)$$

Finally, application of eq 3

$$r_{H-H} = 5.815[T_{1,\mathrm{min(H\cdots H)}}/\nu]^{1/6} \quad (3)$$

gave an estimation of the H···H distance in the dihydrogen-bonded adduct **3a** of 1.66 Å, falling in the typical range of DHB lengths.[1,27]

Reaction of 3 with HFIP. In the presence of 10 equiv of the more acidic HFIP ($pK_a = 9.3$), only the [IrH]···$HOCH(CF_3)_2$ adduct (**3b**) could be observed between 190 and 230 K, with the original peaks of **3** being shifted as in the case of the interaction with TFE [$\Delta\delta_H = -0.4$ ppm; $\Delta\delta_P = -2.1$ ppm, $T_{1,min} = 352$ ms (190 K)]. At variance with our finding with in situ protonation using HBF_4 (vide supra), at 250 K *two* species, **4b′** and **4b″**, were detected. They have NMR parameters very close to those of **4**, obtained from the reaction with HBF_4. **4b′** shows a singlet on the $^{31}P\{^1H\}$ NMR spectrum at −23.7 ppm and a doublet of triplets centered at −11.2 ppm on the hydride region of the ^1H NMR spectrum ($^2J_{H-P(trans)} = 119.3$ Hz; $^2J_{H-P(cis)} = 17.6$ Hz), while **4b″** appears as a singlet at −23.2 ppm on the $^{31}P\{^1H\}$ NMR spectrum and a doublet of triplets (partially overlapped with that of **4b′**) centered at −11.07 ppm on the ^1H NMR ($^2J_{H-P(trans)} = 120.6$ Hz; $^2J_{H-P(cis)} = 18.0$ Hz; Figure 5). The $T_{1,min}$ values found for **4b′** and **4b″** at 250 K are 181 and 177 ms, respectively. The possible chemical nature of both **4b′** and **4b″** are critically discussed with the help of DFT calculations (vide infra). Further warming leads to a gradual signal intensity redistribution, indicating complete conversion of **3** into **4b′**/**4b″**. Leaving the sample at room temperature led to further conversion to the *di*hydride derivative [(κ^4-NP_3)IrH_2][$OCH(CF_3)_2$] (**5b**), which became complete in ca. 18 h. Unlike **5**, obtained by HBF_4 protonation, the ^1H NMR spectrum was well-resolved, and it was possible to observe all of the couplings (Figure 6). Thus, the hydride resonances appear as two well-separated doublets of triplets of doublets centered at −10.6 ppm (H trans to P; $^2J_{H-P(trans)} = 116.1$ Hz; $^2J_{H-P(cis)} = 19.5$ Hz; $^2J_{H-H} = 5.1$ Hz) and −18.4 ppm (H trans to N; $^2J_{H-P(cis1)} = 14.4$ Hz; $^2J_{H-P(cis2)} = 15.0$ Hz; $^2J_{H-H} = 5.1$ Hz), respectively. The $^{31}P\{^1H\}$ NMR pattern is of an AM_2 system similar to that of **5** (Figure S4 in the Supporting Information): a doublet centered at 19.5 ppm (δ_M) and a triplet centered at 18.2 ppm (δ_A, $^2J_{P-P} = 11.7$ Hz) for the two sets of nonequivalent P atoms. Finally, a 2D $^1H-^{31}P$ HETCOR NMR spectrum of the reaction mixture taken at room temperature before completion was also recorded, as additional proof of the proposed assignment (Figure S5 in the Supporting Information).

In good agreement with NMR analysis, the IR spectra of **3** in the presence of 10 equiv of HFIP at 190−230 K in dichloromethane show only the low-frequency shift and the intensity increase of the ν_{Ir-H} band (Figure S6 in the Supporting Information), evidencing once again DHB formation. Above 250 K, a new band appears in the IR spectrum at 2060 cm^1 (Figure 7), which increases slowly with time and/or with temperature. This band is at the position similar to the one observed in the spectra of **3** in the presence of 1 equiv of HBF_4 (under the conditions of complete proton transfer) and is assigned to species **4**.

Theoretical Study of Hydrogen Bonding to 3. DFT optimizations of the various structures described above were carried out, together with frequency calculations, using the model ligand $N(CH_2CH_2PH_2)_3$, where the three PPh_2 ends of the NP_3 ligand have been replaced by PH_2 groups. The functional of choice was Truhlar's M05-2X,[31] specially designed for the computational

(31) (a) Zhao, Y.; Truhlar, D. G. *Theor. Chem. Acc.* **2008**, *120*, 215. (b) Zhao, Y.; Truhlar, D. G. *Acc. Chem. Res.* **2008**, *41*, 157.

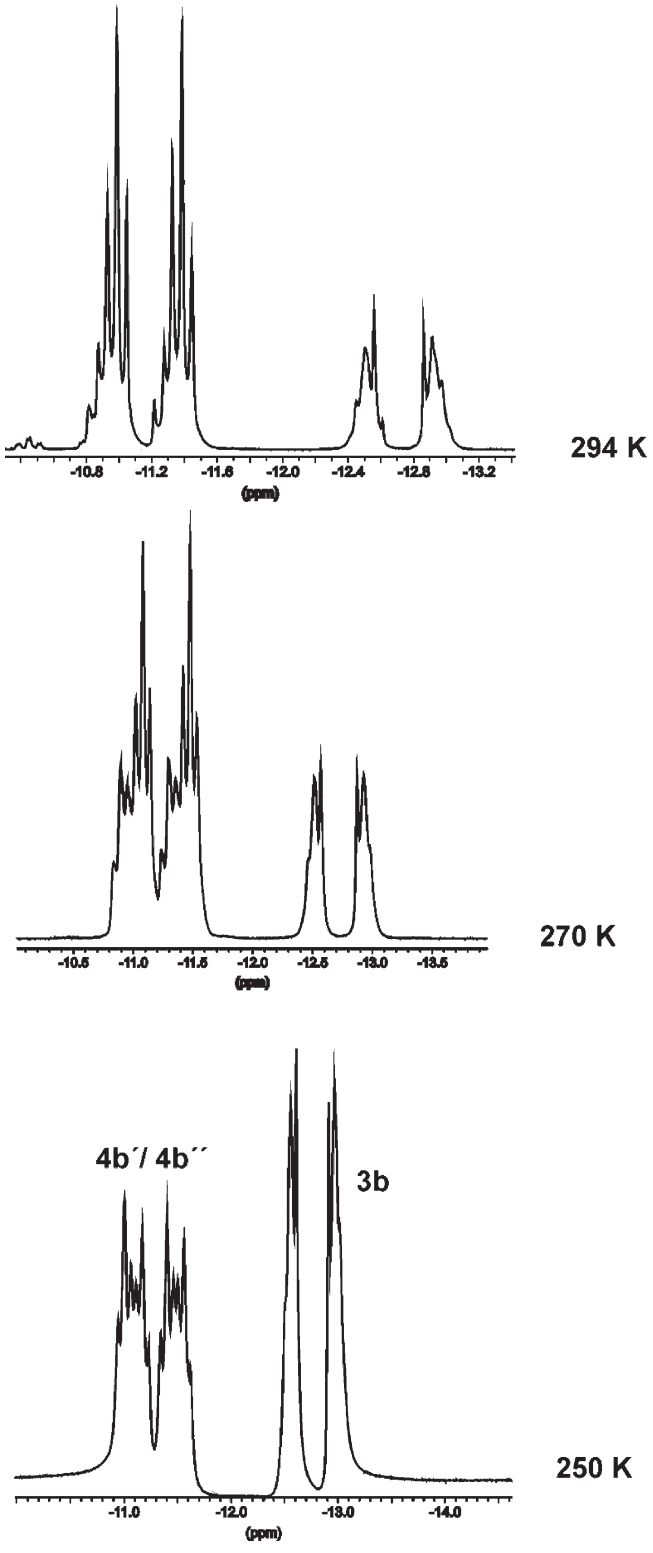

Figure 5. Variable-temperature ^{1}H NMR spectra (hydride region) of the **3**/HFIP (10 equiv) mixture in CD_2Cl_2.

treatment of both third-row transition-metal thermochemistry and general noncovalent interactions (e.g., hydrogen bonding).[32] The optimized Ir−H distance in **3**^{t} is 1.59 Å, while the calculated ν(Ir−H) stretching frequencies are 2228 (fully symmetrical $\nu^1_{Ir-H_3}$), 2197 (ν^2), and 2151 (ν^3) cm^{-1} (for the graphical representation of the Ir−H normal modes and their intensities, see Figure S7 in the Supporting Information). The overestimation with respect to **3** is usual for DFT calculations in the gas phase. The Ir···N separation in **3**^{t} is 3.611 Å, pointing out a good agreement with the X-ray-determined structure of **3** (experimental value of 3.518 Å; see above).

The optimized structure of the DHB adduct between **3**^{t} and TFE (**3a**^{t}; Figure 8a) shows that the proton donor is close to two hydride ligands, interacting more strongly with one of the two. The calculated (O)H···H(Ir) distances are 1.818 and 2.115 Å, and the O−H··H(Ir) angles are 144.4 and 127.8°. Thus, this adduct can be considered as an example of the asymmetric bifurcated dihydrogen-bonded complex. A similar structural motif for DHB species has been theoretically found as the most stable adduct for the interaction of TFE with Cp*Mo(dppe)H$_3$.[7,8] The proton of TFE is slightly below the plane defined by two of the three hydrides and the Ir atom [H−Ir−H−H(O) dihedral angle of −17.0°], leading to a relatively short separation from the Ir atom [$d_{OH\cdots Ir}$ = 2.719 Å; α_{O-H-Ir} = 158.4°]. This arrangement suggests also participation of the metal atom in hydrogen bonding.[7] The **3a**^{t} formation energy is −13.2 kcal mol^{-1} in the gas phase and −5.3 kcal mol^{-1} in dichloromethane. The alcohol ν_{O-H} stretching falls at 3690 cm^{-1} in **3a**^{t}, while in free (optimized) TFE, it appears at 3939 cm^{-1}. The wavenumber decrease in **3a**^{t} is in accordance with a common O−H bond weakening due to hydrogen bond formation. The calculated ν(Ir−H) normal modes have different contributions from different Ir−H bond vibrations (see Figure S6 in the Supporting Information), and two out of three appear at lower frequencies [2224 (ν^1), 2169 (ν^2), 2184 (ν^3) cm^{-1}] in comparison to those of **3**^{t}. This illustrates the difficulty in the interpretation of the spectroscopic changes caused by dihydrogen bonding in the case of polyhydride compounds.

The dihydrogen-bonded adduct between **3**^{t} and HFIP (**3b**^{t}; Figure 8b) shows features very similar to those of **3a**^{t}, although with a stronger interaction, in agreement with the stronger acidity of HFIP. Both the (O)−H···H distance with the closer hydride and the (O)H···Ir distance have decreased (1.722 and 2.605 Å, respectively), whereas the (O)−H···H distance with the second hydride has increased (2.164 Å). The incoming proton is now placed further below the plane defined by the two hydrides and the Ir atom [H−Ir−H−H(O) dihedral angle of −25.9°], pointing toward the Ir−H bond, with $\alpha_{O-H-H(Ir)}$ and α_{O-H-Ir} angles of 163.2 and 159.2°, respectively. The energetic parameters of the HFIP adduct (−15.0 kcal mol^{-1} in the gas phase and −5.4 kcal mol^{-1} in dichloromethane) reflect such a stronger interaction. The calculated ν(Ir−H) vibrations in **3b**^{t} appear at frequencies lower than those in **3a**^{t}: 2218 (ν^1), 2144 (ν^2), and 2113 (ν^3) cm^{-1}. The ν_{OH} stretching falls at 3503 cm^{-1} (in free HFIP, ν_{OH} = 3907 cm^{-1}), with $\Delta\nu_{O-H}$ being much bigger than that in the case of **3a**^{t} (−404 vs −249 cm^{-1}) because of the stronger interaction with a more acidic proton donor. Using these $\Delta\nu_{O-H}$ values, the DHB formation enthalpy can be estimated as −4.6 kcal mol^{-1} for **3a**^{t} and −6.5 kcal mol^{-1} for **3b**^{t} using the known $\Delta\nu_{O-H}/\Delta H$ correlation.[6b,9]

Proton-Transfer Process. Looking at complex **3**, there are five centers that could be susceptible to interaction with proton donors. These are nitrogen, iridium, and the three

(32) (a) Bühl, M.; Reimann, C.; Pantazis, D. A.; Bredow, T.; Neese, F. *J. Chem. Theor. Comput.* **2008**, *4*, 1449. (b) Zhao, Y.; Truhlar, D. G. *J. Chem. Theor. Comput.* **2008**, *4*, 1849. (c) Sousa, S. F.; Fernandes, P. A.; Ramos, M. J. *J. Phys Chem. A* **2007**, *111*, 10439.

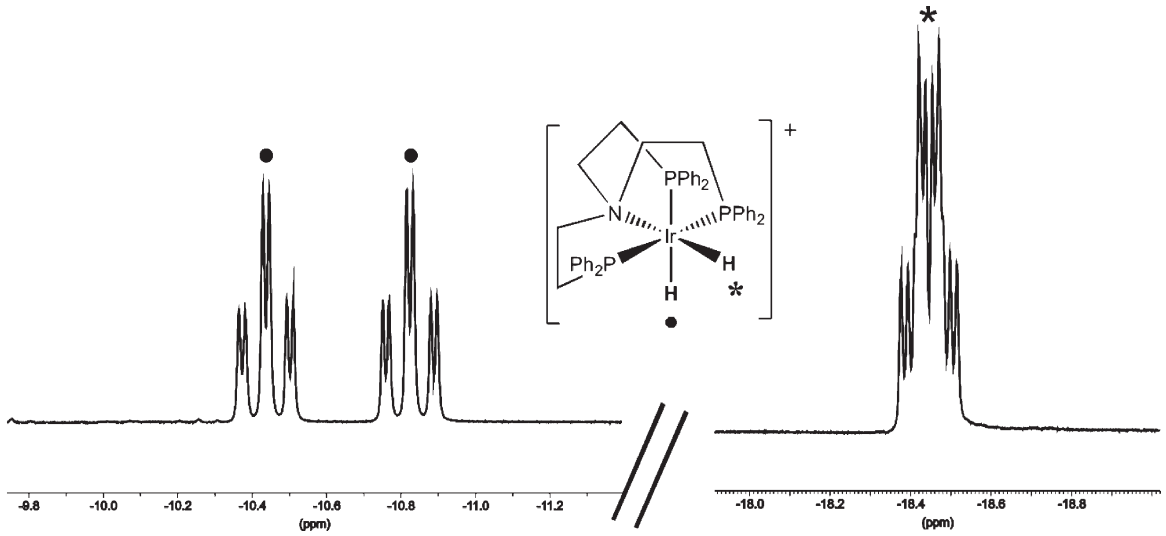

Figure 6. ^{1}H NMR spectrum of **5b** (hydride region only, CD_2Cl_2, 298 K).

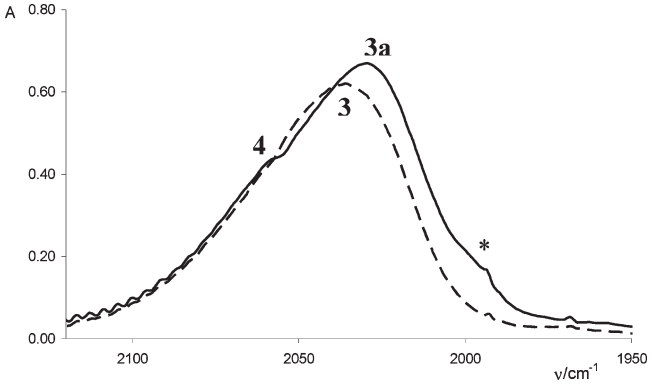

Figure 7. IR spectra (ν_{Ir-H} region) of **3** (0.005 M, dashed line) and of **3** in the presence of 10 equiv of HFIP (solid line). CH_2Cl_2, 270 K. The asterisk indicates a band due to HFIP.

hydride ligands. Inspection of the structure leaves only the last two as suitable candidates for the electrophilic attack because the N atom is located in such a way that its lone pair pointing to the Ir atom is hidden by the ethylene bridges of the NP_3 ligand, in contrast to what happens with chelating aminophosphane ligands such as 1,2-bis[(diisopropylphosphino)amino]ethane (dippae) and 1,2-bis[(diisopropylphosphino)amino]cyclohexane (dippach).[11,14] Such geometry is typical for the κ^3-coordinated NP_3 ligand, as evidenced by the CSD database inspection.[25] Accordingly, the experimental spectroscopic study does not give any evidence of the proton attack at the nitrogen site. A CCSD search revealed only one complex of "protonated" NP_3, [(κ^3-*P*,*P*,*P*-HNP_3)-Ni(CO)]BPh_4, featuring the *inside-oriented* N−H···Ni hydrogen bond, but it was obtained by the reductive intramolecular hydrogen transfer upon CO addition to [(κ^4-NP_3)-NiH]BPh_4 rather than via external proton delivery.[13]

Protonation of **3** with HFIP or HBF_4 gives the tetrahydrido complex **4**, which is, however, not stable at room temperature and loses dihydrogen slowly, yielding **5**. The IR and NMR data obtained for the interaction of **3** with fluorinated alcohols are in agreement with the Ir−H···HOR hydrogen-bond formation preceding the proton transfer. Notably, despite the presence of three hydride ligands, changes in the NMR spectra and a decrease of the $T_{1,min}$ relaxation time in

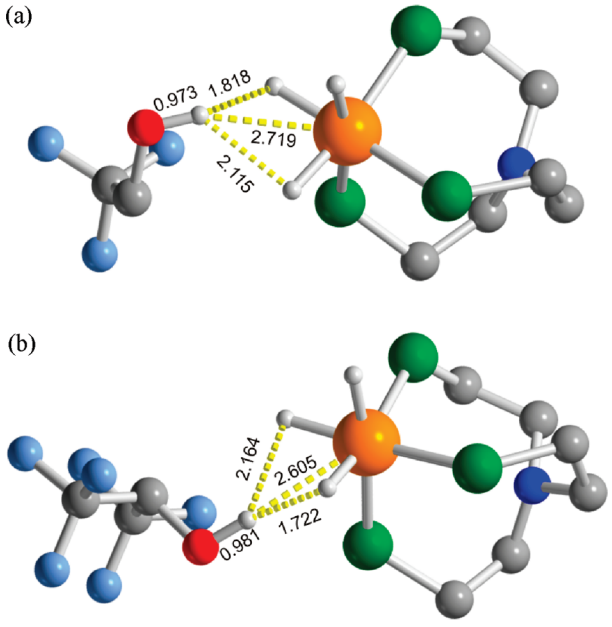

Figure 8. Optimized structures of (a) **3a**^{t} and (b) **3b**^{t}. Selected bond lengths are reported (Å). Atom color code: orange, Ir; white, H; red, O; blue, N; gray, C; green, P; light blue, F. H atoms on the $N(CH_2CH_2PH_2)_3$ ligand and on the alcohols are omitted for clarity. The short contacts are depicted in yellow (dotted lines).

the presence of alcohol are clearly observable for these systems, in contrast with what was found for [Cp*MH_3-(dppe)]···HOR complexes.[7,9]

The assignment of a well-defined structure to iridium polyhydrides is a very difficult task, and the structure of L_3IrH_4 complexes has been a matter of debate, leading to the conclusion that these species generally deny any simple characterization in terms of individual well-defined structures.[33−35] The highly fluxional behavior of the

(33) Gutiérrez-Puebla, E.; Monge, A.; Paneque, M.; Poveda, M. L.; Taboada, S.; Trujillo, M.; Carmona, E. *J. Am. Chem. Soc.* **1999**, *121*, 346.
(34) Webster, C. E.; Singleton, D. A.; Szymanski, M. J.; Hall, M. B.; Zhao, C.; Jia, G.; Lin, Z. *J. Am. Chem. Soc.* **2001**, *123*, 9822.
(35) Hebden, T. J.; Goldberg, K. I.; Heinekey, D. M.; Zhang, X.; Emge, T. J.; Goldman, A. S.; Krogh-Jespersen, K. *Inorg. Chem.* **2010**, *49*, 1733.

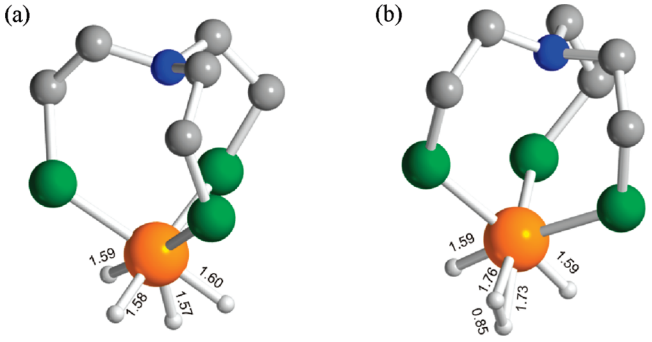

Figure 9. Optimized structures of (a) **TETRA** and (b) **DIH**. Selected bond lengths reported (Å). Atom color code: see Figure 8. H atoms on the $N(CH_2CH_2PH_2)_3$ ligand are omitted for clarity.

hydrogen ligands does not help, and the use of the T_1 criterion may only lead to ambiguous or even incorrect conclusions.[36] From ^1H and ^2H NMR observations, hydridotris(pyrazolyl)boratoiridum tetrahydride ($TpIrH_4$) has been proposed to be a classical tetrahydride species with a C_{3v} structure, in which a hydride ligand is capping the IrH_3 face.[33] Afterward, DFT optimizations and high-level ab initio calculations of $TpIrH_4$ have found two minimum-energy structures almost isoenergetic: a C_s edge-bridged octahedral structure, with the fourth hydride sitting on an $Ir(H)_2$ edge, and a C_1 η^2-dihydrogen dihydride structure.[34] The presence of both a dihydrogen ligand and two classical hydrides in $[(triphos)IrH_4]^+$ [triphos = $MeC(CH_2PPh_2)_3$][37] and in *cis*,*trans*-$[Ir(4\text{-}C_5NF_4)H_4(P^iPr_3)_2]$ (4-C_5NF_4 = 2,3,5,6-tetrafluoro-4-pyridyl) has been deduced from NMR T_1 measurements and isotopic labeling with deuterium.[38] Anyway, these compounds appear as highly fluxional species because of the fast hydride exchange processes.[39]

We carried out DFT calculations to determine the structure of the protonation product **4**, bearing in mind that different species are observed on both ^1H and $^{31}P\{^1H\}$ NMR spectra depending on the acid used. Two minima were located, closely related to those previously found for the $TpIrH_4$ complexes (Figure 9).[34] In the first one, the incoming H atom is placed on a $Ir(H)_2$ edge in a pseudoplane with the other two hydrides and two P atoms of the NP_3 ligand. The complex can be described as a pentagonal-bipyramidal classical tetrahydrido species $[\{\kappa^3\text{-}P,P,P\text{-}N(CH_2CH_2PH_2)_3\}IrH_4]^+$ (**TETRA**), although the short distance between the fourth H atom and one hydride (1.417 Å) allows also its description as a compressed dihydride.[40,41] The second minimum is an octahedral mixed classical−nonclassical compound $[\{\kappa^3\text{-}P,P,P\text{-}N(CH_2CH_2PH_2)_3\}Ir(\eta^2\text{-}H_2)(H)_2]^+$ (**DIH**). The presence of a dihydrogen ligand is indisputable in this tautomer from the calculated H−H distance of 0.85 Å. As in $TpIrH_4$[34] and (PCP)IrH_4[35] [PCP = κ^3-1,3-$(CH_2P^tBu_2)_2$-C_6H_3], the two forms are almost isoenergetic [ΔE(**DIH-TETRA**) = −0.4 kcal mol^{-1} (gas phase)/−0.5 kcal mol^{-1} (CH_2Cl_2), with the **DIH** isomer being slightly more stable], precluding any discrimination between **DIH** and **TETRA**. The Ir−H stretching vibration frequencies calculated for these two isomers do not allow for discrimination between the two species either. For **TETRA**, ν_{Ir-H} appears at 2363 (ν^1), 2252 (ν^2), 2247 (ν^3), and 2219 (ν^4) cm^{-1}, with the latter one being the most intense. In **DIH**, vibrations of the $Ir(\eta^2\text{-}H_2)$ moiety are rather weak, whereas vibrations of two terminal hydride ligands ($\nu^s_{Ir-H_2}$ = 2254 and $\nu^{as}_{Ir-H_2}$ = 2225 cm^{-1}) fall in the same region as ν^2−ν^4 of **TETRA** and are of comparable intensity to ν^4 (see the Supporting Information for more details).

In order to check if other isomers could be stable geometries on the potential energy surface (PES), optimizations starting from different structures were carried out. The bis-dihydrogen $[\{\kappa^3\text{-}P,P,P\text{-}N(CH_2CH_2PH_2)_3\}Ir(\eta^2\text{-}H_2)_2]^+$ led to **TETRA** during optimization, while the end-on coordination of the η^1-bound dihydrogen in $\{[\kappa^3\text{-}P,P,P\text{-}N(CH_2CH_2PH_2)_3\}Ir(\eta^1\text{-}H_2)(H)_2]^+$ converted into **DIH**. The possibility of a $[H_3]^+$ ligand was theoretically and experimentally considered in the 1980s.[42] In our case, optimization of an initial pseudoallylic geometry $[\{\kappa^3\text{-}P,P,P\text{-}N(CH_2CH_2PH_2)_3\}Ir(\eta^3\text{-}H_3)(H)\}^+$ led again to **TETRA**. Therefore, none of them represents a stable structure at the computational level used.

The theoretical data cannot clearly discriminate between the two almost isoenergetic species **DIH** and **TETRA**, which are located on an extremely flat energy surface. Furthermore, the hypothetical alcoholate neutral complex $[\{\kappa^3\text{-}P,P,P\text{-}N(CH_2CH_2PH_2)_3\}Ir(OR)(H)_2]$, where the counterion acts as a ligand on iridium(III), has to be discarded because its formation is energetically unfavorable. In fact, the internal energy variation (calculated in CH_2Cl_2) associated with the reaction

$$\mathbf{3^t} + HFIP \rightarrow [\{\kappa^3\text{-}P,P,P\text{-}N(CH_2CH_2PH_2)_3\}Ir(OR)(H)_2\} + H_2 \quad (4)$$

equals to +12.7 kcal mol^{-1}, while that of the $\mathbf{3^t}$ + HFIP → $\mathbf{3b^t}$ reaction is *negative*: − 5.4 kcal mol^{-1}. The formation of homoconjugated pair species $[\{\kappa^3\text{-}P,P,P\text{-}N(CH_2CH_2PH_2)_3\}IrH_4](OR)\cdot nROH$, where the excess of free alcohol may form a hydrogen-bonded counterion $[R{-}O\cdots H{-}OR]^-$ or $[R{-}O\cdots(H{-}OR)_n]^-$ instead of the simple alcoholate RO^-, has been shown by IR and NMR methods for CF_3COOH or *p*-nitrophenol interacting with hydrides,[30d,e,43,44] but it is difficult to be proved for HFIP, which does not have any suitable spectroscopic label.

(36) (a) Gusev, D. G.; Kuhlman, R. L.; Renkema, K. B.; Eisenstein, O.; Caulton, K. G. *Inorg. Chem.* **1996**, *35*, 6775. (b) Desroisiers, P. J.; Cai, L.; Lin, Z.; Richards, R.; Halpern, J. *J. Am. Chem. Soc.* **1991**, *113*, 4173. (c) Gusev, D. G.; Hübener, R.; Burger, P.; Orama, O.; Berke, H. *J. Am. Chem. Soc.* **1997**, *119*, 3716.
(37) Bianchini, C.; Moneti, S.; Peruzzini, M.; Vizza, F. *Inorg. Chem.* **1997**, *36*, 5818.
(38) Salomon, M. A.; Braun, T.; Krossing, I. *Dalton Trans.* **2008**, 5197.
(39) Maseras, F.; Lledós, A.; Clot, E.; Eisenstein, O. *Chem. Rev.* **2000**, *100*, 601.
(40) (a) Gelabert, R.; Moreno, M.; Lluch, J. M.; Lledós, A.; Pons, V.; Heinekey, D. M. *J. Am. Chem. Soc.* **2004**, *126*, 8813. (b) Gelabert, R.; Moreno, M.; Lluch, J. M.; Lledós, A.; Heinekey, D. M. *J. Am. Chem. Soc.* **2005**, *127*, 5632.
(41) Heinekey, D. M.; Lledós, A.; Lluch, J. M. *Chem. Soc. Rev.* **2004**, *33*, 175.
(42) (a) Burdett, J. K.; Pourian, M. R. *Inorg. Chem.* **1988**, *27*, 4445. (b) Heinekey, D. M.; Payne, N. G.; Schulte, G. K. *J. Am. Chem. Soc.* **1988**, *110*, 2303.
(43) Belkova, N. V.; Besora, M.; Epstein, L. M.; Lledós, A.; Maseras, F.; Shubina, E. S. *J. Am. Chem. Soc.* **2003**, *125*, 7715.
(44) Belkova, N. V.; Collange, E.; Dub, P.; Epstein, L. M.; Lemenovskii, D. A.; Lledós, A.; Maresca, O.; Maseras, F.; Poli, R.; Revin, P. O.; Shubina, E. S.; Vorontsov, E. V. *Chem.—Eur. J.* **2005**, *11*, 873.

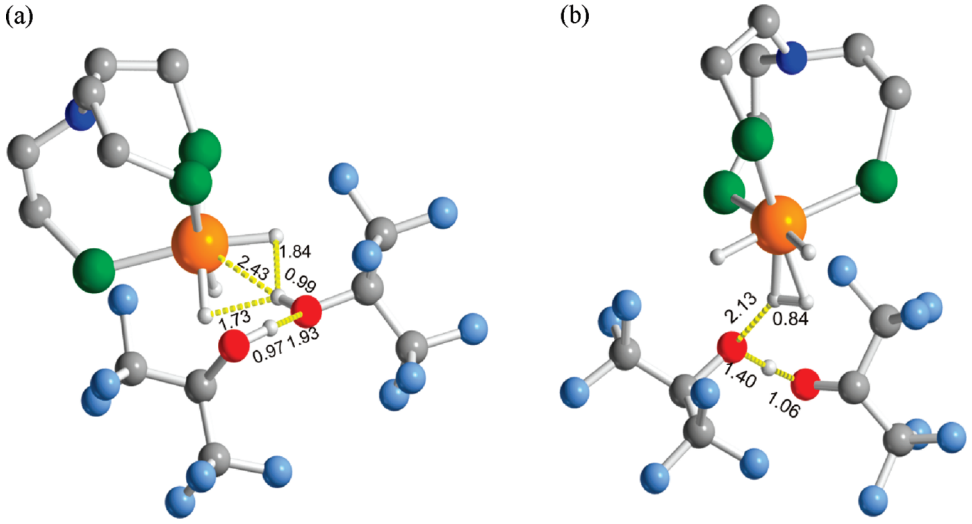

Figure 10. Optimized structures of (a) $\mathbf{3^t}\cdots\mathbf{(HFIP)_2}$ and (b) the proton-transfer product **DIH**·[**AHA**]. Selected bond lengths reported (Å). Atom color code: see Figure 8. H atoms on the $N(CH_2CH_2PH_2)_3$ ligand are omitted for clarity.

The involvement of two alcohol molecules in the proton-transfer process has been suggested for the $[Cp^*RuH_3(PCy_3)]$/HFIP system[45] and confirmed by kinetic studies for $[Cp^*FeH(dppe)]$ protonation by different alcohols.[44,46] Binding of additional alcohol molecules would alter the $[\{\kappa^3\text{-}P,P,P\text{-}N(CH_2CH_2PH_2)_3\}IrH_4](OR)$ ion-pair stability (weakening the IrH···OR interaction, whose presence is clearly indicated by the dependence of the hydride signal position on the HFIP concentration) but not the cation nature/structure, which agrees with both the similarity of the ^{1}H NMR chemical shift and the multiplicity of **4b′**/**4b″**. Surprisingly, the optimization of nonclassical and classical cation structures in the presence of a $[(CF_3)_2CHO\cdots HOCH(CF_3)_2]^-$ anion, **DIH**·[**AHA**] and **TETRA**·[**AHA**], gave in both cases the dihydrido dihydrogen cation bonded with the homoconjugated HFIP anion (**DIH**·[**AHA**]; Figure 10b). Thus, in the presence of the counteranion, only the dihydrogen dihydride isomer would be stable. The similar effect of the counteranion favoring the nonclassical structure was obtained very recently for the $[Cp^*Mo(CO)(PMe_3)_2(H_2)]BF_4$ system in a parallel study by some of us.[47]

The energy barrier for the occurrence of the proton-transfer reaction was also evaluated, starting from the $\mathbf{3^t}\cdots\mathbf{(HFIP)_2}$ system (Figure 10a) and analyzing its internal energy variation (evaluated in CH_2Cl_2; single-point calculation with the BS2 basis set on the BS1-optimized geometries) with the d_{O-H} reaction coordinate, as performed in similar literature cases.[7,44] In the starting geometry, $d_{(O-H)opt}$ = 0.994 Å; a maximum was found for d_{O-H} = 2.7 Å, 19.5 kcal mol^{-1} above the reagents. The final proton-transfer product is $\Delta E = +16.0$ kcal mol^{-1}. The values so obtained are much lower than those in the gas phase (energetic barrier = 27.3 kcal mol^{-1}; thermodynamic ΔE = +21.1 kcal mol^{-1}), as expected, mirroring the trend found in the literature.[7,44]

Scheme 3

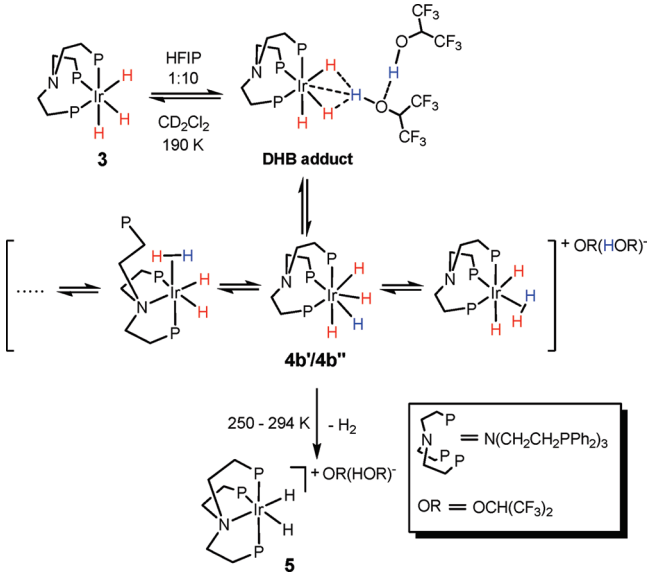

From all of these results and in keeping with the negligible energy differences between the computed species, a rationale for the reaction mechanism accounting for protonation of **3** may be the following: it starts with dihydrogen-bonded adduct formation, followed by protonation of one Ir−H bond to give the tetrahydride **4**. In the case of HBF_4 protonation, when only one set of resonances appears in the low-temperature spectrum, it is impossible to discriminate between the classical tetrahydride and the nonclassical dihydrido dihydrogen complex cation. However, on the basis of T_1 arguments (vide supra), the lack of hydrogen-bonding network capabilities of the BF_4^- anion, and literature data,[37] it is conceivable that the rapidly exchanging tetrahydride tautomer is preferred, although no final decision can be taken. A similar degree of uncertainty also stands in the case of HFIP protonation (Scheme 3), where the situation is further complicated by the appearance of two similar sets of resonances on the ^{1}H NMR spectrum, which slowly transforms into the κ^4-NP_3 dihydride **5**. From careful

(45) Gründemann, S.; Ulrich, S.; Limbach, H.-H.; Golubev, N.; Denisov, G. S.; Epstein, L. M.; Sabo-Etienne, S.; Chaudret, B. *Inorg. Chem.* **1999**, *38*, 2550.

(46) Belkova, N. V.; Revin, P. O.; Epstein, L. M.; Vorontsov, E. V.; Bakhmutov, V. I.; Shubina, E. S.; Collange, E.; Poli, R. *J. Am. Chem. Soc.* **2003**, *125*, 11106.

(47) Dub, P. A.; Belkova, N. V.; Filippov, O. A.; Daran, J.-C.; Epstein, L. M.; Lledós, A.; Shubina, E. S.; Poli, R. *Chem.—Eur. J.* **2010**, *16*, 189.

examination of the whole body of collected experimental and theoretical information, we are inclined to suppose that, after formation of an initial DHB adduct [corresponding to the DFT minimum $\mathbf{3^t\cdots(HFIP)_2}$], the conformational flexibility of the NP_3 ligand could allow for an easy coordination mode "switch" from κ^3-*P*,*P*,*P*-NP_3 to κ^3-*P*,*P*,*N*-NP_3, as confirmed by additional theoretical evidence coming from a PES scan along the d_{Ir-N} reaction coordinate. In fact, starting from either the **TETRA** or **DIH**·[**AHA**] geometry and shortening the Ir−N distance, which entails concomitant N-coordination, *a simultaneous* $-PH_2$ *detachment* is observed, maintaining the octahedral coordination geometry on the iridium center and leaving one "dangling" NP_3 arm (Figure S8 in the Supporting Information). The energy of this tautomer is 1.6 kcal mol^{-1} *below*(!) that of **DIH**·[**AHA**] in dichloromethane, and the small energy difference favors the existence of an equilibrium between the two isomers. No stable geometry corresponding to either eight-coordinated $[(\kappa^4\text{-}NP_3)IrH_4]^+$ or seven-coordinated $[(\kappa^4\text{-}NP_3)Ir(\eta^2\text{-}H_2)(H)_2]^+$ was found, despite the fact similar species were characterized in the case of rhenium.[28] As soon as the temperature is raised from 250 to 294 K, the κ^4-NP_3 mode is prevalent, and subsequent loss of molecular dihydrogen from the intermediate(s) generates **5** as the only stable product observed at ambient temperature after 18 h.[48]

Conclusions

The novel trihydride **3** has been synthesized and characterized through IR/multinuclear NMR spectrometry and X-ray diffraction. Treatment with strong (HBF_4) and medium-strength (TFE and HFIP) proton donors showed that DHB formation precedes hydride protonation to yield the species **4**, whose nature has been critically examined with the help of DFT calculations. Discrimination between a classical and nonclassical hydride cannot be made on the basis of the DFT results for the "naked" cations, but in the presence of the $[(CF_3)_2CHO\cdots HOCH(CF_3)_2]^-$ counteranion, only the dihydrogen/dihydride isomer seems to be stable. The final loss of molecular dihydrogen at room temperature gives **5**. In the reaction of **3** with the medium-strength acid HFIP, two distinct intermediates, **4b′** and **4b″**, are observed on the low-temperature ^1H NMR spectra, having very similar $T_{1,min}$ values, δ_H, and related coupling patterns (doublet of triplets). An unambiguous assignment of their identity is impossible on the basis of the collected data; this is not surprising, in view of the extensive literature on related iridium tetrahydrides, where it is always hard to discriminate between different tautomers.[33−35] In the present case, the high flexibility of the NP_3 backbone, with the κ^3-P,P,N-coordination isomer slightly more stable than the κ^3-P,P,P one, together with the easy switching between the κ^3 and κ^4 hapticities, further complicates the situation, vanishing every attempt of a definite and clear description.

Acknowledgment. The work was supported by the RFBR (Grant 08-03-00464) and CNR-RAS bilateral agreement. The motu proprio FIRENZE HYDROLAB project by Ente Cassa di Risparmio di Firenze (http://www.iccom.cnr.it/hydrolab/) and the PIRODE project by MATTM (Rome) are kindly acknowledged for funding of this research activity also through a postdoctoral grant to A.R. Thanks are also expressed to the GDRE project "Homogeneous Catalysis for Sustainable Development". A.L. thanks the Spanish MICINN (Projects CTQ2008-06866-C02-01 and ORFEO Consolider Ingenio 2010 CSD2007-00006). The use of the computational facilities of the Centre de Supercomputació de Catalunya (CESCA) is greatly appreciated.

Supporting Information Available: Figures S1−S8, crystallographic tables for **1**, and Cartesian coordinates and absolute energies (in the gas phase and in dichloromethane) of the optimized geometries of $\mathbf{3^t}$, $\mathbf{5^t}$, $\mathbf{3a^t}$, $\mathbf{3b^t}$, **TETRA**, **DIH**, $\mathbf{3^t\cdots(HFIP)_2}$, **DIH**·[**AHA**], and (κ^3-*P*,*P*,*N*-NP_3)-**DIH**[**AHA**]. This material is available free of charge via the Internet at http://pubs.acs.org.

(48) In $\mathbf{5^t}$, the two hydride ligands appear to be totally independent: $\nu^1_{Ir-1H} = 2188\ cm^{-1}$, $\nu^2_{Ir-1H} = 2368\ cm^{-1}$.